La mer 51：93-106, 2013
Société franco-japonaise d'océanographie, Tokyo

Numerical simulation on sedimentation in Yangon River and its navigation channel

TOE TOE AUNG[1)*], Takenori. SHIMOZONO and Akio. OKAYASU[*]

Abstract： A shallow area called, Inner Bar, near Yangon Port is a major obstacle for Yangon River traffic. In order to obtain basic information for the sedimentation problem, characteristics of flow, sediment transport and bed level changes were investigated for Yangon River and its navigation channel by means of numerical simulation. 3–D Princeton Ocean Model (POM) with a wetting and drying scheme was used to cope with large tidal ranges for predicting the river and tidal flows. Topographic data, upstream river discharges and tidal elevations at the river mouth were given as the input data for the models. Computed depth-averaged velocity was verified against field data of NELSON (2000). Bed shear stress was evaluated from bottom velocity calculated by the 3–D flow model. Bed level change was simulated with a 2–D sediment transport model for different seasonal and tidal conditions. Sediment diameter used in the calculation was obtained by sand sampling from material of Inner Bar. The simulation clearly showed large amount of sand deposition at Inner Bar and some other areas in the river. Estimated amount of sedimentation around Inner Bar was roughly equivalent to that of bottom material dredged by Myanmar Port Authority to maintain the depth.

Keywords： *Yangon River, sedimentation, numerical calculation, tide, wetting and drying*

1. Introduction

Sedimentation in rivers and estuaries is a common problem for maintenance of waterways. The river fresh water and daily or twice-daily reversing flows due to tidal action make flows in estuaries and tidal section of rivers complex. Fig. 1 shows the area of interest for the present study, the Yangon River which is on an eastern branch of Ayeyarwaddy River. The Ayeyarwaddy River is the fifth largest in the world in terms of sediment discharge, depositing more than 360 million tons of sediment annually into the continental shelf in the

1) Phone: 95–1–556375;
Email: toetoeoung@gmail.com
*Corresponding author:
Coastal Environment and Engineering Laboratory, Department of Ocean Sciences, Tokyo University of Marine Science and Technology,
4–5–7. Konan, Minato, Tokyo 108–8477, Japan
Phone: 03–5463–0473; Fax: 03–5463–0517
Email: okayasu@kaiyodai.ac.jp

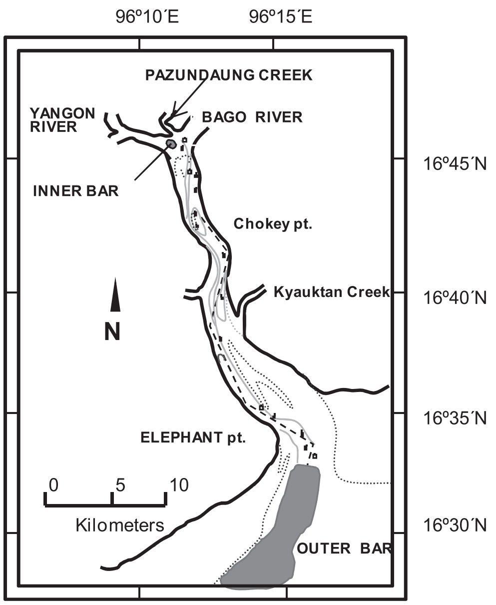

Fig. 1. Locations of Yangon River and Estuary and the two sand bars, Inner Bar and Outer Bar

northern Andaman Sea. Yangon River is the most important river to Myanmar for 90% of its international marine trades are transported through this channel. The distance between the Yangon Port and the river mouth is about 45 kilometers and the width of river in the region is from 2 kilometers to 7 kilometers. Active sediment transport due to river flows and tidal currents causes two major shallow water areas; one is called “Inner Bar” located inside the river near Yangon Port and the other is “Outer Bar” which extends out from the river mouth as shown in Fig. 1. Dredging works are required to maintain depth of the channel at these areas. Despite knowledge gathered on the Yangon River and Estuary system, little information is currently available on the behavior of sediment transport caused by the river flow and the tidal currents. Therefore it is difficult to take effective measures for sedimentation other than dredging.

There were some researches focused on the problem due to sedimentation at shallow water areas in Yangon River. SIR ALEXANDER GIBB and PARTNERS (1974) investigated physical conditions of Yangon River through an extensive field study. NELSON (2000) conducted a field study on the behavior of fine-grained sediment in Yangon River by measuring the current speed, depth, salinity and sediment concentration. CHINA TRANSPORTATION ENGINEERING (2006) made a proposal on an improvement of the conflux of the Yangon River, Pazundaung Creek and the Bago River. They proposed three types of dikes for controlling the main flow. TOE TOE AUNG *et al.* (2011) computed flows and sediment transport in Yangon River by a 2–D numerical model. In their paper, sediment transport was simulated from depth-averaged velocity given by the 2D flow model and sediment particle size (8 to 50 μm and the mean diameter is 11 μm) used in the calculation was based on the results of field study by SIR ALEXANDER GIBB and PARTNERS (1974), where actual sediment diameter at Inner Bar was much larger than that used in the calculation.

Although near-bottom velocity generally gives a dominant effect to sediment transport, most of the previous studies didn’t consider three dimensionality of the flow field. Since the tidal range in the area is very large, dry-up of the river bottom should also be considered in the calculation. In this study, 3–D Princeton Ocean Model with the wetting and drying scheme was used for flow evaluation to obtain the near bed velocity fields which are important both for bed load and suspended sediment transport. Sediment diameter of interest is another important factor for evaluation of sediment transport. Thus, a field observation was carried out to obtain the sediment diameter of which forms the shallow area at Inner Bar.

Then, 2–D sediment transport has been computed by using the calculated bottom velocity and water surface elevation resulted from the flow model and the sediment diameter obtained from the field observation described above. It was assumed in the present study that near-bottom sediment transport is dominant also for suspended sediment transport. Thus velocity calculated by the 3–D flow model for the bottom layer was used to evaluate suspended load in the 2–D sediment transport model. The deposition rate of sediment at Inner Bar was evaluated and compared with the amount of dredging conducted by Myanmar Port Authority.

2. MODEL DESCRIPTIONS

2.1 Flow model

The 3–D Princeton Ocean Model (POM) with a wetting and drying scheme was used for the investigation of flow characteristics in Yangon River. The Princeton Ocean Model (POM) is a three-dimensional, primitive equation, numerical ocean model, mainly used for solving the hydrodynamics in the coastal region and bays and estuaries (BLUMBERG and MELLOR, 1987). The POM employs a finite difference scheme to numerically solve the primitive equations. The model is calculated with external and internal modes; the external mode portion of the model has short time steps for the 2–DH flow field and the internal mode has long time steps to evaluate its vertical distribution. The horizontal finite difference grids can be rectangular (as used in this study) or curvilinear orthogonal, while the vertical grids are in sigma coordinates which are the normalized vertical coordinates with the water column depth. The use of sigma levels gives better resolution of the boundary layers. Detailed information on the formulation and derivation of these equations including the definitions for each variable and formulas for the specific terms in these equations were included in the POM User's Guide (MELLOR, 2004).

POM08 with wetting and drying (WAD) scheme (OEY, 2005) was used in this study among versions of POM. Wetting and drying process was considered to account for the dry up areas due to high tidal ranges. For the use of WAD scheme, it is necessary to define the absolute land boundary (ALB) which must be high enough in elevation, so that water can never split into that area. In the land side of ALB, the area was always dry and the land mask FSM (time-independent land mask) and WADMASK (time-dependent mask for wet and dry condition) are set to be 0. Toward the seaward of the ALB, FSM is 1 and WADMASK was 1 or 0 depending on whether the cell is wet or dry (OEY, 2006). In Oey's WAD scheme, a minimum depth (dry depth=5 cm) is defined to determine the "dry" or "wet" state of each cell. When the total depth (D), which is the summation of water depth (H) and elevation (η), falls below the minimum depth, cells are considered as dry.

In this study, ALB were located along the river bank so that the water did not flood over the bank because the bank slope was relatively steep and the actual flood distance due to high tides were smaller than a grid size. The wet and dry process was calculated only for shoals within the river channels. Based on the Oey's scheme, the calculation was done with dry depth of 5 cm as the minimum depth to calculate velocity. 5 cm was set as the lowest limit for calculation and if the water depth was less than 5 cm, the corresponding flux was set as zero. From the results of the flow model in the study area shown in Fig. 6, it can be seen that WAD scheme is capable of calculating well for high tidal condition in the study area as illustrated in Fig.7. Without WAD scheme, computations break down at the ebb tide due to the large tidal range.

Simulations were made for two different seasons, the monsoon and the dry season, since the seasonal variation of river discharge was significant. Moreover, the simulation was carried out on two tide conditions; spring tide with a tidal range of 5.2 m and neap tide, 1.8 m. Therefore the model was run for four cases (Table 2); spring tide at monsoon and dry season and neap tide at monsoon and dry season. Before computing the sediment transport, the Shields parameter was calculated by using the bottom velocity results from the flow model and the sediment particle sizes obtained from field study described in Chapter 3. From distributions of Shields parameter calculated for each case, possible sediment deposition areas can be estimated with a sediment transport model.

2.2 Sediment Transport Model

The velocity and water depth were interpolated from the results of the flow model for the required time step according to the courant number and used as input data for sediment transport model. The governing equation for the suspended sediment transport is the advection-diffusion equation with the entrainment and deposition terms,

$$\frac{\partial(CD)}{\partial t}+\frac{\partial(uCD)}{\partial x}+\frac{\partial(vCD)}{\partial y}=\frac{\partial}{\partial x}\left(\varepsilon D\frac{\partial C}{\partial x}\right)+\frac{\partial}{\partial y}\left(\varepsilon D\frac{\partial C}{\partial y}\right)+\omega_s(E_s-\overline{C}_b) \qquad (1)$$

Symbol t is time, D is total water depth, ε is eddy viscosity, u and v are the velocity components in x and y direction, ω_s is settling velocity of sediment in water, C is depth-averaged sediment concentration, $\overline{C}_b$ is near bed concentration and E_s is dimensionless rate of sediment into suspension across unit area per unit time. As described in the previous section, velocity at the bottom layer is used for evaluation of suspended load in the present study.

The eddy viscosity is calculated by LANE and KALINSKE (1941) as

$$\varepsilon = 1/D\int_0^D \varepsilon(Z)dz = u_* KD/6 \qquad (2)$$

where u_* is the shear velocity at the bed and K is the Karman constant. The entrainment of sediment is calculated by the formula of GARCIA and PARKER (1993),

$$E_s = \frac{AZ_U^5}{1+\frac{\alpha}{0.3}Z_U^5} \tag{3}$$

$$A = 1.37\times10^{-7}, Z_U = (u^*/\omega_s)^5 R_{ep}^3,$$

$$R_{ep} = \sqrt{RgD_s^3}/v, R = (\rho_s/\rho)-1.$$

where R_{ep} is particle Reynolds number, ρ_s, ρ are density of sediment particle and water, υ is the kinematic viscosity of water, D_s is diameter of sediment particle. The settling velocity ω_s is calculated by the formula of CHENG (1997).

$$\frac{\omega_s D_s}{v} = \left(\sqrt{25+1.2d_*^2}-5\right)^{1.5} \tag{4}$$

where,

$$d_* = \left(\frac{Rg}{v^2}\right)^{1/3} D_s \tag{5}$$

By assuming a vertical distribution of sediment concentration to be Rousean profile (ROUSE, 1937), the near bed concentration is evaluated by $C_b=\gamma_0\ C$. PARKER *et al.* (1987) gave a simple fit to the profile and derived the following expression for γ_0,

$$\gamma_0 = 1+31.5\left(\frac{u_*}{\omega_s}\right)^{-1.46} \tag{6}$$

By the combination of suspended sediment and bed load, the bed level change, Z_b is calculated by the bottom evolution equation

$$(1-\lambda_p)\frac{\partial Z_b}{\partial t} = -\frac{\partial q_{bx}}{\partial x}-\frac{\partial q_{by}}{\partial y}+\omega_s(\overline{C}_b-E_s) \tag{7}$$

λ_p is the bed porosity. The bed load transport q_{bx}, q_{by} is evaluated by the Meyer-Peter and Muller equation (MEYER-PETER and MULLER, 1948)

$$q_b = 8\sqrt{\left(\frac{\rho_s}{\rho}-1\right)gD_s^3}\,(\tau_*-\tau_{*c})^{\frac{3}{2}} \tag{8}$$

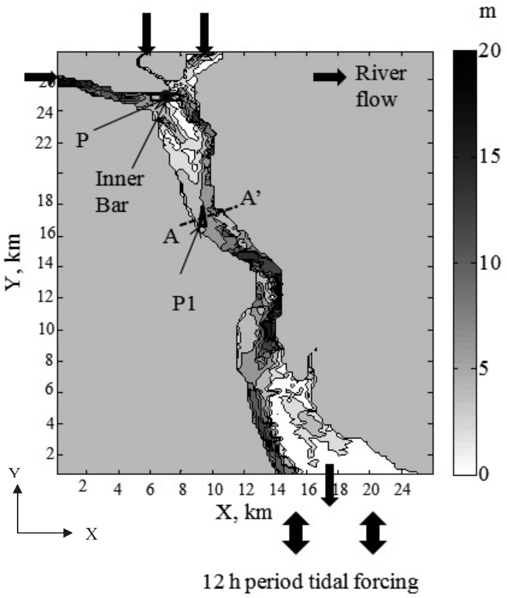

Fig. 2. Bathymetry of Yangon River and boundary elements for calculation. Section A-A' shows the location of field survey conducted by NELSON (2000). P shows one of the point in the Inner Bar and P1 indicates the location for velocity comparisons given in Fig. 5. (The datum of bathymetry is the lowest low water level.)

$\tau_*$and τ_{*c} are the base shear stress and critical shear stress. The MacCormack Scheme is used for discretization (FENNEMA. and CHAUDHRY, 1990).

2.3 Input Data and Boundary Conditions

Bathymetry, discharge of the three rivers and the tidal elevation at the river mouth were given to the flow model as the input data. The calculating area of the Yangon River lies between 16°30′N to 16°47′N latitude and 96°10′E to 96°20′E longitude. The bathymetry data was created by digitizing the sounding chart provided by MYANMAR PORT AUTHORITY (2007) shown in Fig. 2. The grid spacing was 6 seconds for both latitude and longitude (approximately 170 meters at the site) and 6 vertical sigma levels were determined. The external time step in the flow model was 1 s and the internal time step was 4 s according to Courant-Fredrics-Levy (CFL) condition. The discharge data of

Table 1. Discharge data of three rivers in dry and monsoon (rainy) seasons

	Dry Season (m^3/s)	Monsoon Season (m^3/s)
Yangon River	627	6853
Pazundaung Creek	143	866
Bago River	315	1566

Fig. 3. Dredging ship and bottom material (mixture of sand and water) taken from Inner Bar (16° 45.817′N and 96°11.945′E) on 16th September 2010.

three rivers for dry and monsoon seasons were shown in Table 1. These discharge data were from the field data of Sir Alexander Gibb and Partners (1974). The tidal range varied between 5.2 m and 1.8 m near the city of Yangon (Myanmar Port Authority).

The present computational domain had three up-stream inflows and an outflow boundary at the river mouth as shown in Fig. 2. Estimated discharges of the upper three rivers were constantly given at the inflow boundaries while the sum of them was discharged from the outflow boundary. For the tidal current, water surface elevation and the corresponding tidal velocity were given at the outflow boundary assuming in a form of sinusoidal waves. To simplify the model, the temperature and salinity which supposed to be less important for bed level change in rivers were kept constant during the simulation.

For sediment concentration, the inlet of the three rivers and outlet of the river were assumed to be in equilibrium state for given flow velocities. Sediment diameter was set at 0.338 mm based on the field result obtained for the Inner Bar as described below.

3. Sampling of Sedimentation Material

Particle size is one of the most important parameters for sediment transport. Since amount of sediment transport is greatly affected by sediment diameter, an appropriate sediment diameter should be chosen to evaluate sedimentation at Inner Bar. In the previous studies, sediment diameter in the Yangon River system was only given for suspended sediment (e.g. Sir Alexander Gibb and Partners, 1974) whose representative diameter is usually much different from that for bed materials.

In order to give an appropriate grain size of bed materials to the numerical model, field observation was conducted at the Inner Bar area in Yangon River on 16 September 2010. Sediment sample was taken from bed materials on a dredging ship (Fig. 3) being operated to dredge sediment deposited at Inner Bar.

The distribution of particle diameters was obtained by the sieve analysis for the bed material. Although it was observed that the suspended sediment sampled near river surface was composed of very fine sand, clay and silt with diameters ranging from several μm to a hundred μm, the bed material from Inner Bar had d_{75} diameter of 0.338 mm which was much larger than the suspended material. The grain size distribution curve for the bed material is shown in Fig. 4. Therefore in the present study, diameter of 0.338 mm is used as the representative sediment diameter for the bed materials in order to evaluate sand movement causing Inner Bar sedimentation.

Table 2. Four conditions of calculation in terms of tidal rage and river discharges.

	Monsoon	Dry
Spring tide (5.2 m tidal height)	Case 1	Case 2
Neap tide (1.8 m tidal height)	Case 3	Case 4

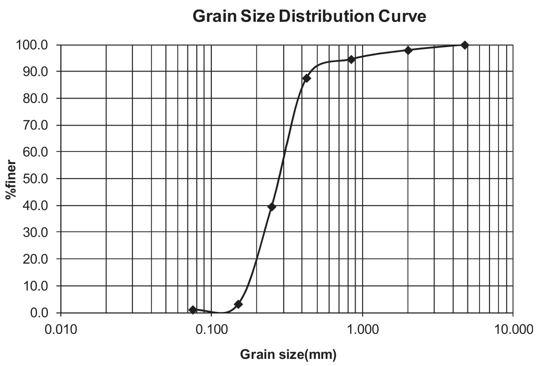

Fig. 4. Grain size distribution curve for bed material from the Inner Bar Area.

4. Results and Discussions

4.1 Calculated depth-averaged flow field and comparison with field data

Flow velocity for spring tide at monsoon season (Case 1 in Table 2) is shown in Fig. 5. Fig. 5. (a) and (b) give the depth-averaged velocity fields at the ebb and the flood tide conditions for spring tide at monsoon season, respectively. During ebb tide, the flow direction is seaward. During flood tide, the flow was directed towards the upstream of the river, since the river discharge only had a limited influence to the overall flow pattern. Comparisons of the surface and bottom flow velocity at ebb and flood tide conditions show that the bottom velocity is generally smaller than the surface velocity but the flow directions and patterns are similar.

To verify the numerical simulation, the cal-

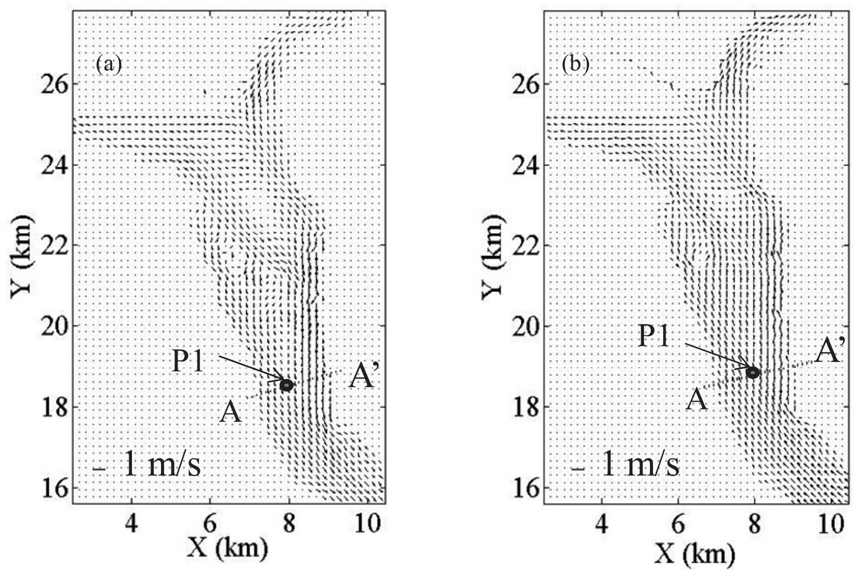

Fig. 5. The depth-averaged velocity fields for (a) ebb tide and (b) flood tide at spring tide during the monsoon season

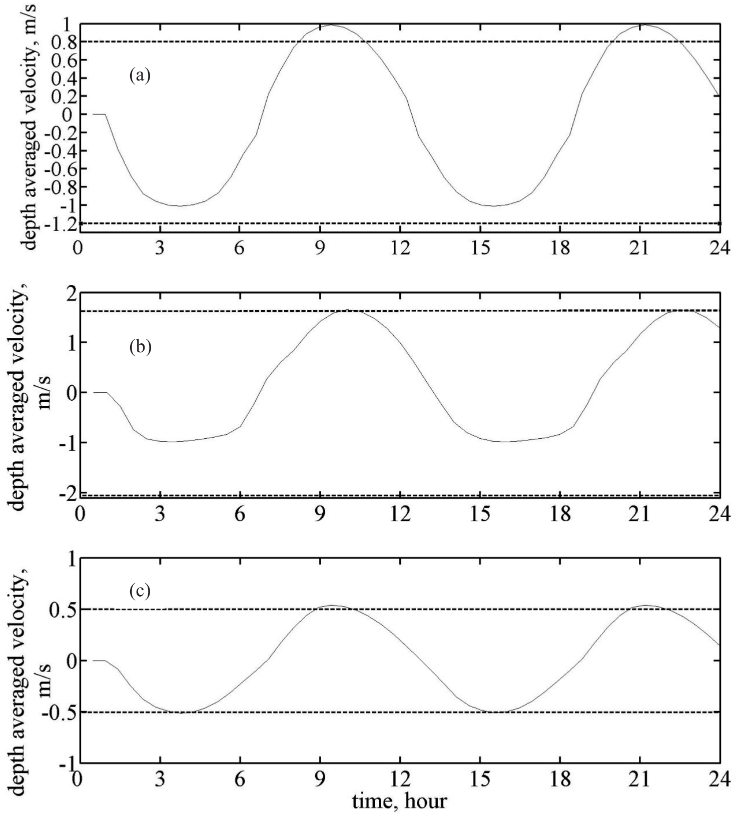

Fig. 6. The depth-average velocity for (a) spring tide in the monsoon season, (b) spring tide in the dry season and (c) neap tide in the dry season at point P1. The dotted lines show the field results of NELSON (2000). (The lines with positive values are at flood tide condition and those with negative values are at ebb tide condition.)

culated depth-averaged velocities were compared with field results obtained by NELSON (2000) at the 10 km downstream of the Yangon Port (A-A' cross section in Fig. 5). The simulation was done for three conditions; the spring tide in monsoon season, the spring tide in dry season and the neap tide in dry season according to the conditions for Nelson. The field observation of Nelson gave the maximum depth-averaged velocity for the spring tide in monsoon season and the neap tide in dry season. But for the spring tide in dry season, it gave only one value for velocity and did not mention whether it was depth-averaged velocity or maximum velocity.

Time variations of depth-averaged velocity calculated at P1 indicated in Fig.5 are shown in Fig. 6, although information of the exact measurement location is not provided in NELSON (2000). The dotted straight lines correspond to the values of depth-averaged velocities obtained by Nelson. The model results of the spring tide in monsoon season and the neap tide in dry season are in good agreement with the field data. In the case of spring tide at dry season, the model result for flood tide velocity is nearly equivalent with the field result but the model result for ebb tide velocity is smaller than the field measurement. The discrepancy might occur due to the lack of information of the exact locations of the field study area. Since the difference is found in the ebb tide condition, another possible reason can be the river discharge which might be larger at the time of

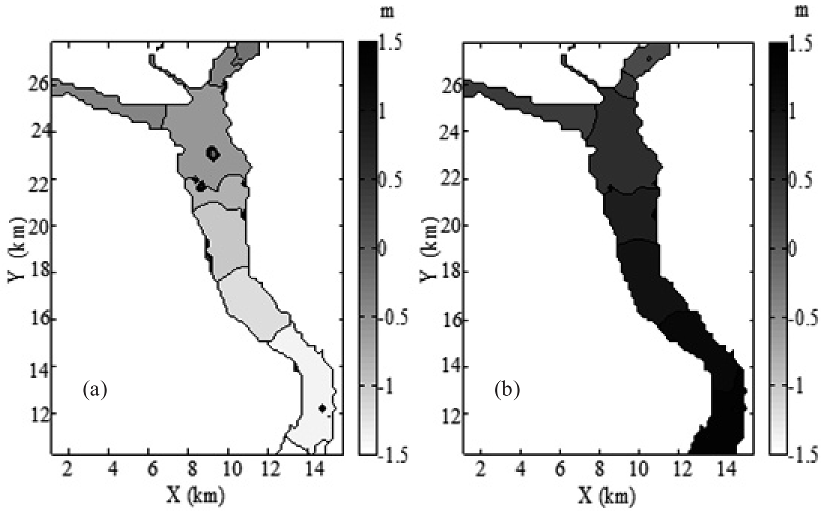

Fig. 7. The water surface elevation with respect to the mean sea level (m) for (a) ebb tide and (b) flood tide. The dried areas are shown as the water surface elevation is 0.

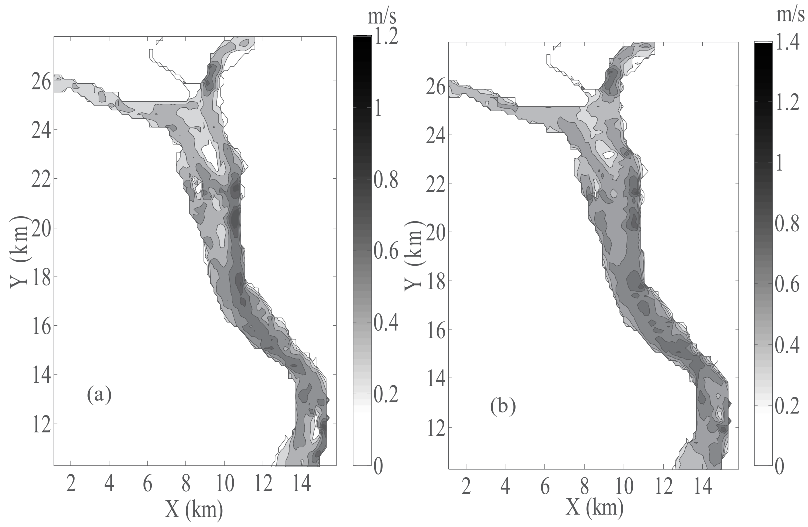

Fig. 8. The magnitude of depth-averaged velocity (m/s) for (a) ebb tide and (b) flood tide.

measurement. The river discharge used in present model was from SIR ALEXANDER GIBB and PARTNERS (1974) which were older than NELSON (2000).

4.2 Results and Discussions for flow model

The velocity fields, depth-averaged velocity and velocity for each layer of depth, water surface elevation with respect to the mean sea level at the ebb and flood tide conditions were obtained respectively for the four cases listed in Table 2.

The results on the spring tide at monsoon season (Case 1 in Table 2) are shown in Fig. 7 and 8. Fig. 7 (a) and (b) show the water surface elevation for ebb and flood tide conditions, respectively. Some dry areas where the water surface elevation is expressed as 0 for practical

Table 3. Calculated bottom velocity and resulting Shields parameters at Inner Bar which is indicated by symbol "P" in Fig. 1.

Period	Tidal Forcing	Tidal condition	Bottom Velocity (m/s)	Shields Parameter
Monsoon	Spring	Flood	0.55	0.0091
		Ebb	0.45	0.0084
	Neap	Flood	0.24	0.0022
		Ebb	0.23	0.0017
Dry	Spring	Flood	0.44	0.0073
		Ebb	0.41	0.005
	Neap	Flood	0.082	0.0002
		Ebb	0.078	0.0002

purpose can be observed clearly in the ebb tide condition while flood water filled up the dry area. Fig.8 (a) and (b) show the magnitude of depth-averaged velocity values for ebb and flood tide conditions, respectively. The largest velocity occurred in the downstream of the Yangon River and the magnitude of the depth-averaged velocity during ebb tide and flood tide were up to 1.7 m/s. The magnitude of depth-averaged velocity takes its minimum near the junction of the three rivers as well as the places associated with the shallow water areas. This might be because flows from rivers with different directions met each other at the junction and some parts of their velocities cancelled each other out.

The model results in the monsoon and dry seasons for one of the point (indicated by P in Fig. 2) near Inner Bar area under both of the spring and neap tide conditions are shown in Table 3 together with Shields parameter calculated for sand diameter of 0.338 mm. It can be seen that the bottom velocities of flood tide were slightly larger than those of the ebb tide for all cases. The resulting values of the Shields parameter near Inner Bar area were very small and indicate that sediment deposition should occur around the area.

The results of the other three cases, Case 2, 3 and 4, are not shown in the figures but gave similar characteristic with Case 1. For water surface elevation, dry-up areas were calculated during ebb tide condition in very shallow areas. The depth-averaged velocities for Case 2 (neap tide at monsoon season) were varying from 0.2 to 0.6 m/s. For Case 3 (spring tide at dry season), the velocities were about 0.4 to 1.5 m/s. It was found that the magnitudes of depth-averaged velocity were about 0.1 to 0.5 m/s in Case 4 (neap tide condition at dry season).

4.3 Sediment Transport and Bathymetry Change

Calculations for sediment transport were performed for the four cases given in Table 2. The ratio of the suspended load and bed load transports in the calculation around the Inner Bar area was roughly evaluated as 9 : 1. The combined results of suspended load and bed load transports are used in the calculation of bed level change and the evaluated bed level changes are shown in Figs. 9 to 12. In each figure, sub-figure (a) and (b) represent the accumulated bed level changes for one ebb tide (a half of one tidal cycle) and one flood tide and sub-figures (c) represent those for one whole tidal cycle. The zero value represents the initial river bed and negative values represent erosion and positive values are for deposition. From the results, it is found that the deposition and erosion are larger in spring tide conditions than those in neap tide conditions for both monsoon and dry seasons. Please note that the scales for sedimentation are different between the figures for spring tide conditions (Figs. 9 and 10) and those for neap tide conditions (Figs. 11 and 12).

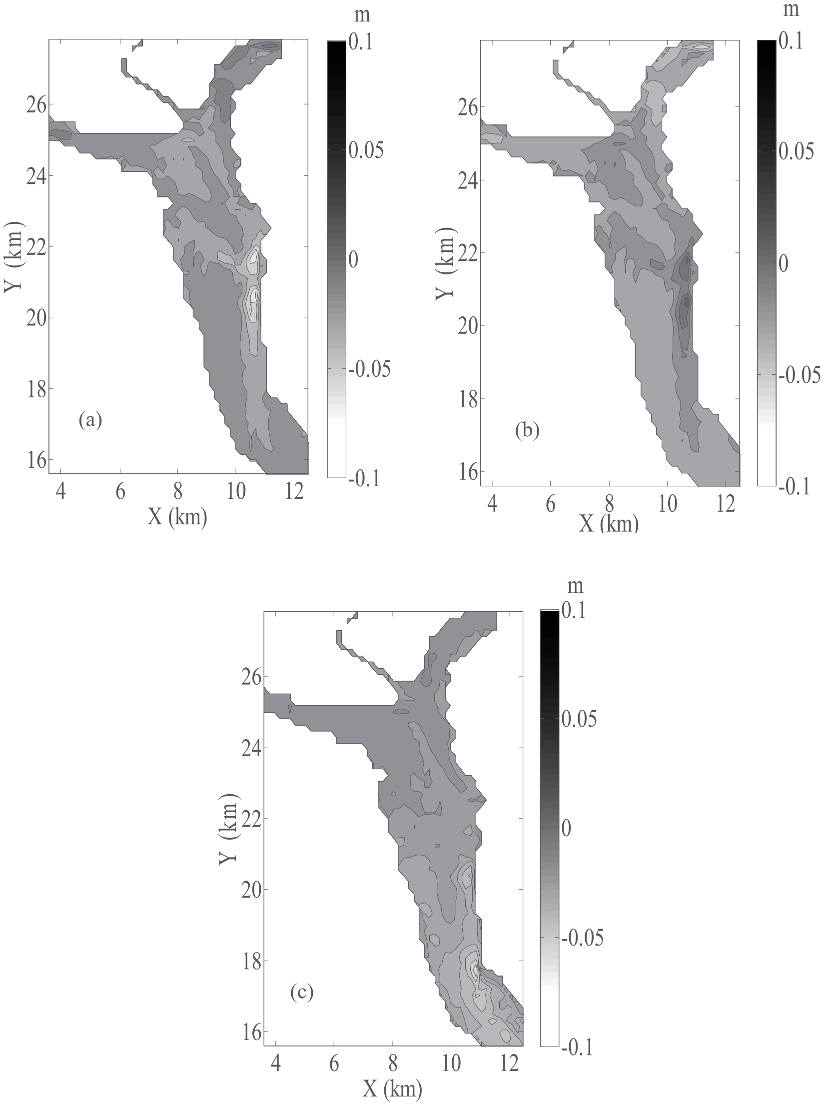

Fig. 9. Accumulated bed level change (m) for (a) ebb tide and (b) flood tide condition and (c) one tidal cycle at spring tide at monsoon season.

The results indicated that the deposition occurred around Inner Bar (indicated by the symbol P in Fig. 2) for all the cases. Remarkable deposition is seen just at Inner Bar for the case of spring tide at monsoon season (Fig. 9 (c)) in particular. In other areas, sediment deposition and erosion patterns are consistent with our preexisting knowledge such as other sand bar areas out of the navigation channel and the downstream around the Chokey Point (see Fig. 1) area where erosion occurs in both monsoon and dry seasons.

To maintain the required depth of the navigation channel, Myanmar Port Authority (MPA) does dredging operation by a dredging ship every day. The capacity of the dredging ship is approximately 1000 m^3 and it gets sand of four to six times of its capacity per day near

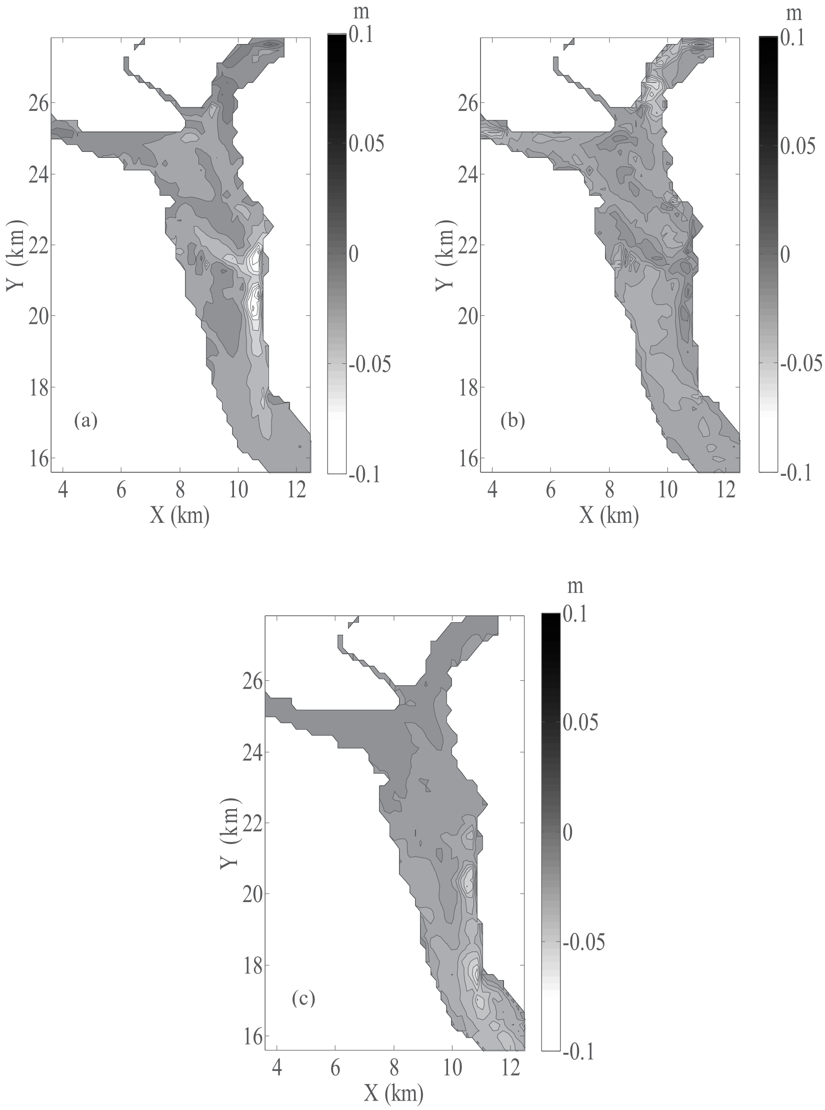

Fig. 10. Accumulated bed level change (m) for (a) ebb tide and (b) flood tide condition and (c) one tidal cycle at spring tide at dry season.

the Inner Bar area. Although it is difficult to estimate the exact volume of dredged material, the amount of it is roughly estimated as 6×10^3 m^3 per day.

From the calculation, rate of deposition at Inner Bar is evaluated to be around 0.04 m per day. If the area of Inner Bar is assumed to be about 1.4×10^5 m^2 (roughly estimated as 1400 m by 100 m from the dredging area and the bathymetry), the amount of sand deposition in a day in the spring tide at monsoon season is estimated by multiplying deposition depth to the estimated Inner Bar area and it was about 6×10^3 m^3 which is equivalent to that obtained by the dredging amount. As the calculated rate of deposition at neap tide conditions is much smaller, about 2×10^3 m^3 per day, the overall evaluation of sedimentation should

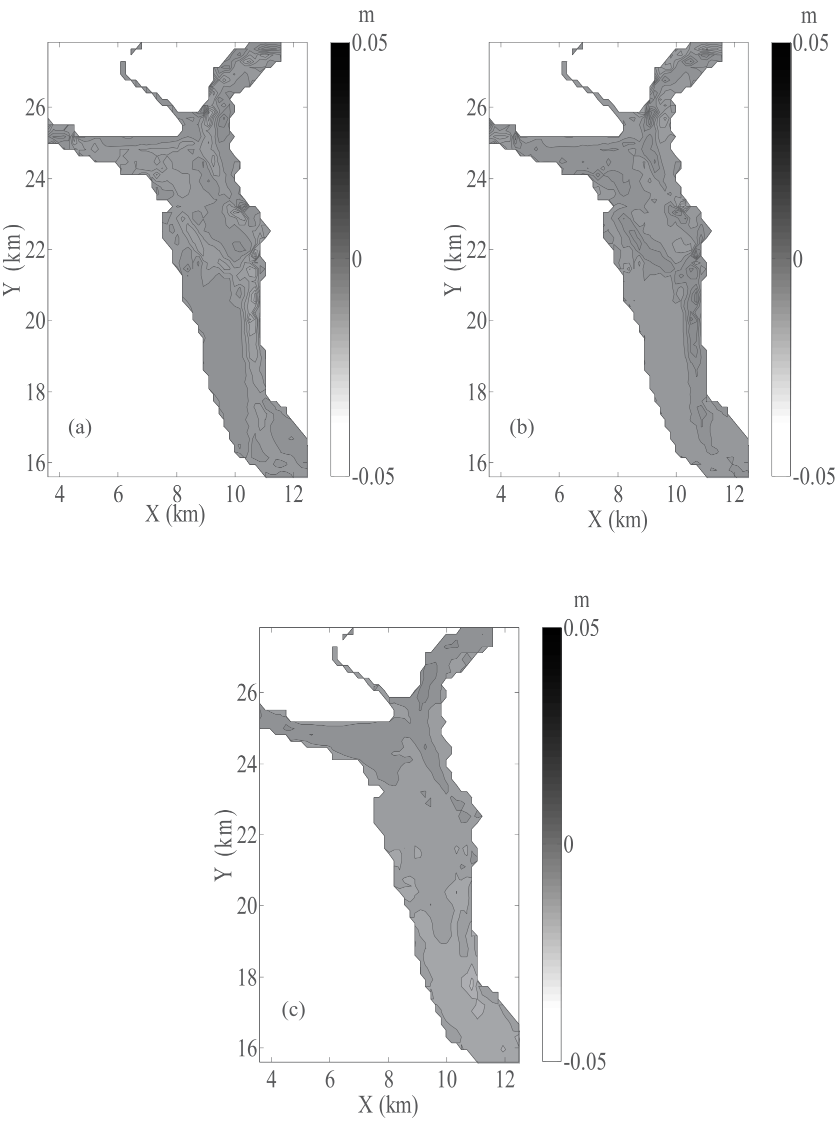

Fig. 11. Accumulated bed level change (m) for (a) ebb tide and (b) flood tide condition and (c) one tidal cycle at neap tide at monsoon season.

be much less. It can however be concluded that the model evaluation of sedimentation is fairly good.

5. Conclusion

In the present study, characteristics of flow fields and resultant sediment transport were investigated by numerical simulation for the navigation channel in Yangon River. The flow fields were evaluated by using the 3-D Princeton Ocean Model (POM) with a wetting and drying scheme to evaluate near-bottom velocity in very shallow areas. It was found that the velocity at flood tide was generally larger than that at ebb tide. Along the navigation channel, velocity was larger at downstream of the river, however, smaller near the junction of the three rivers, Yangon River, Pazundaung Creek and

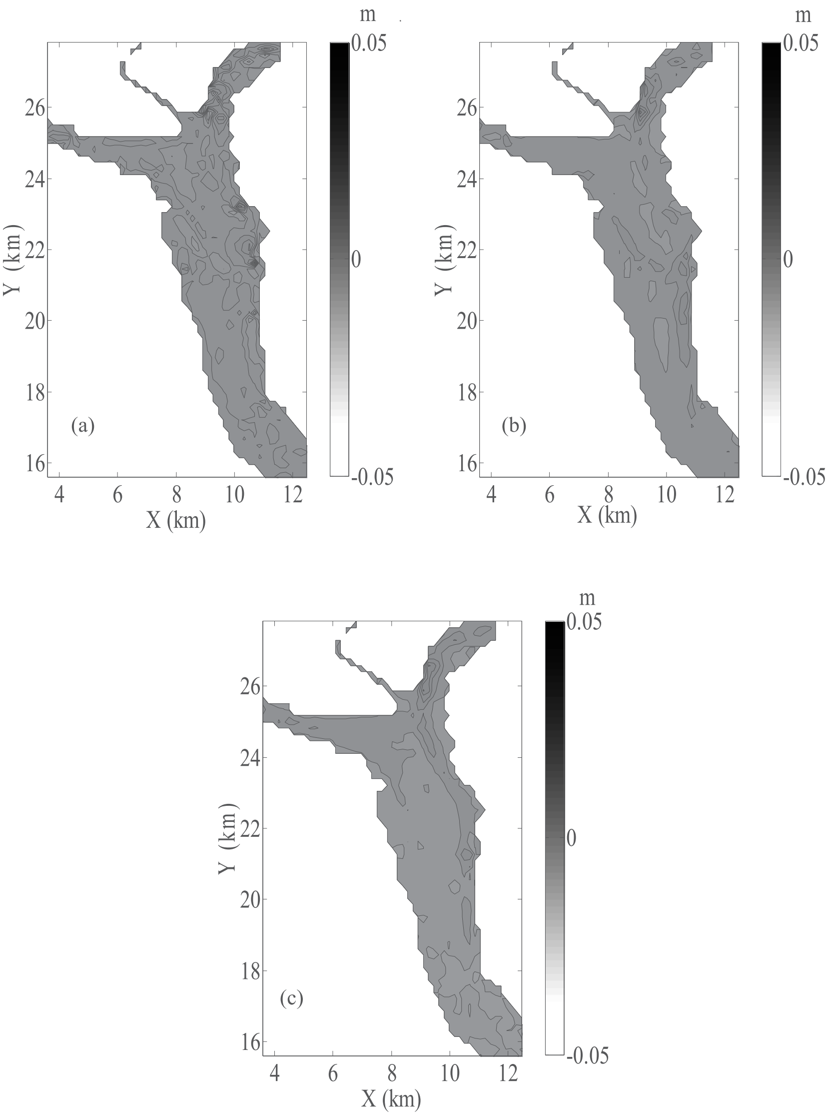

Fig. 12. Accumulated bed level change (m) for (a) ebb tide and (b) flood tide condition and (c) one tidal cycle at neap tide at dry season.

the Bago River where the Inner Bar exists. The calculated velocity showed the reasonable agreement with the field data of NELSON (2000).

Calculated near-bottom velocity was put into the sediment transport model to evaluate sediment deposition and erosion in the channel. From field observation, d_{75} sand diameter for the Inner Bar material was 0.338 mm, which was used in the sediment transport calculation. In all tide and seasonal conditions, sand deposition is observed around the Inner Bar area. It was found that the sedimentation occurs more heavily at the spring tide condition than the neap tide condition. Thus it can be concluded that the present simulation reflects the basic mechanisms of flow and sediment transport around the navigation channel in Yangon

River and can reproduce the actual sand deposition at the Inner Bar fairly well.

The numerical model is expected to be a powerful predictive tool for considering a new measure to maintain the navigation channel and the depth around the port areas in Yangon River. In the further, more reliable field data would be however needed not only for providing accurate conditions for calculation, but also for the verification of the model results.

Acknowledgements

This research was supported by the Ministry of Education, Culture, Sports, Science and Technology (Monbukagakusho: MEXT) of Japan through a Student Research Scholarship Grant awarded to the first author.

References

Blumberg, A. F. and G. L. Mellor (1987): A description of a three-dimensional coastal ocean circulation Model. Three-Dimensional Coastal Ocean Models, **4**, 208–223.

Cheng, N.S. (1997): A simplified settling velocity formula for sediment particle. J. Hydraulic Eng. ASCE, **123**, 149–152.

China Transportation Engineering (2006): Myanmar Yangon River access channel improvement project, Shanghai China.

Fennema, R. J. and M. H. Chaudhry (1990): Explicit methods for 2–D transient free surface flows. J. Hydraulic Eng. ASCE, **116**, 1013–1034.

Garcia, M. and G. Parker (1993): Experiments on the entrainment of sediment into suspension by a dense bottom current. J. of Geophysical Research (Oceans), AGU, **98**, 4793–4807.

Lane, E.W. and A.A. Kalinske (1941): Engineering calculations of suspended sediment. Trans. Amer., Geophy. Union, **20**, 603–607.

Meyer-Peter, E. and R. Muller (1948): Formulas for bed-load transport. Proc., 2nd Meeting, IAHR, 39–64.

Mellor, G. L. (2004): User Guide to A Three-Dimensional, Primitive Equation, Numerical Ocean Model. Princeton University Press, Princeton, 56pp.

Nelson, B. W. (2000): Sediment dynamics in Rangoon River, Myanmar. The Science of Total Environment, **266**, 15–21.

Oey, L. (2005): A wetting and drying scheme for POM. Ocean Modeling, **9**, 133–150.

Oey, L. (2006): An OGCM with movable land-sea boundaries. Ocean Modeling, **13**, 176– 195.

Parker, G., M. H. Garcia, Y. Fukushima and W. Yu (1987): Experiments on turbidity currents over an erodible bed. J. of Hydraulic Research, **25**, 123–147.

Rouse, H. (1937): Experiments on the Mechanics of Sediment Suspension. Proceeding of the 5th International Congress for Applied Mechanics, **55**, 550–554.

Sir Alexander Gibb and Partners (1974): Rangoon sea access channel & associated port improvement Study, United Nations Development Programme: International Bank for Reconstruction and Development: Burma Port Corporation.

Toe Toe Aung, T. Shimozono and A. Okayasu (2011): Numerical study of sediment transport in Yangon River and estuary. Asian and Pacific Coasts 2011, 1509–1516.

Received: June 14, 2013
Accepted: October 25, 2013